Stepwise Solvation Enthalpies of Protonated Water Clusters: Collision-Induced Dissociation as an Alternative to Equilibrium Studies

N. F. Dalleska, Kenji Honma,† and P. B. Armentrout*

Contribution from the Department of Chemistry, University of Utah, Salt Lake City, Utah 84112

Received July 12, 1993®

Abstract: Absolute reaction cross sections for interaction of $H_3O^+(H_2O)_x$ (x = 1-5) with xenon are determined from thermal energies to 20 eV (CM) by using guided ion beam mass spectrometry. In all cases, the primary product is endothermic collision induced dissociation (CID) to lose one water molecule. At higher energies, additional water molecules are lost successively, indicating that evaporation is the primary pathway for dissociation. The proper interpretation of the primary CID thresholds is considered in detail and the adjustment of these values to enthalpies at standard conditions is discussed. When the effects of multiple ion-molecule collisions, internal energy of the clusters, and dissociation lifetimes are properly accounted for, we determine the following bond dissociation energies (in eV): $D_0[H_3O^+-H_2O]$ = 1.35 ± 0.06, $D_0[H_5O_2^+-H_2O]$ = 0.86 ± 0.06, $D_0[H_7O_3^+-H_2O]$ = 0.71 ± 0.06, $D_0[H_9O_4^+-H_2O]$ = 0.52 ± 0.06, and $D_0[H_{11}O_5^+-H_2O]$ = 0.51 ± 0.08. These results are in very good agreement with enthalpies of solvation determined by equilibrium methods.

Introduction

The energetics of water clustering around the proton in the gas phase has been studied extensively.[1-13] Because discrete numbers of water molecules solvating the proton can be studied directly in the gas phase, such a system provides a stepwise model for solvation of the proton in liquid water. In addition, a thorough understanding of these systems is important to atmospheric chemistry, as was realized after the discovery of proton bound water clusters in the upper atmosphere by Narcisi and Bailey in 1965.[14]

Much of what is known about these clusters centers around the enthalpy, $\Delta H°(x)$, and entropy, $\Delta S°(x)$, changes of reaction 1 at 298 K.

$$H_3O^+(H_2O)_x \rightarrow H_3O^+(H_2O)_{x-1} + H_2O \qquad (1)$$

To date, reliable measurements of the enthalpies of hydration for x = 1-5 (listed in Table I) have been performed *exclusively* by high-pressure mass spectrometry (HPMS) and pulsed high-pressure mass spectrometry (PHPMS). Kebarle pioneered these studies by using first HPMS[1] and later PHPMS.[2,3] Kebarle[4] suggests his most reliable values are from Cunningham, Payzant, and Kebarle (CPK)[2] for x = 1 and 2 and from Lau, Ikuta, and Kebarle (LIK)[3] for x = 3-5. Continuous ionization HPMS experiments done by Beggs and Field (BF)[5] initially showed considerable disagreement with Kebarle, but Meot-Ner and Field (MF)[6] and Meot-Ner and Speller (MS)[7] have reproduced the results of Kebarle using PHPMS techniques. Hiraoka, Takimoto, and Yamabe (HTY)[8] reported PHPMS results nearly concurrently with MS. They obtained a significantly higher value of $\Delta H°(1)$ but good agreement for $\Delta H°(2)$. HTY have attributed the discrepancy in $\Delta H°(1)$ to temperature measurement problems associated with the work of Kebarle and co-workers. Some support for a higher value of $\Delta H°(1)$ comes from ab initio calculations of Frisch et al. (FDBS),[9] who find a value of 35.0 kcal/mol with an uncertainty estimated to be less than 2 kcal/mol.

MS provided a complete comparison of known $\Delta H°(x)$ and $\Delta S°(x)$ for reaction 1 and a wide variety of similar molecular cluster systems. At that time, there was generally good agreement between the results of MS and Kebarle, and the few discrepancies with the work of BF and MF could be rationalized after the fact. The centerpiece of MS's analysis is the search for a solvent shell effect as evaluated by the quantity $\delta\Delta H°(x) = \Delta H°(x-1) +$

Table I. Literature Values of $\Delta H°(x)$ (kcal/mol) at 298 K[a]

	x =				
source	1	2	3	4	5
KSZSA[b]	36.0(1.0)	22.3(1.0)	17.0(1.0)	15.3(1.0)	13.0(1.0)
CPK[c]	31.6(1.0)	19.5(1.0)			
LIK[d]			17.9(1.0)	12.7(1.0)	11.6(1.0)
MF[e]	33.0(1.0)	21.0(1.0)	16.0(1.0)		
MS[f]	31.8(1.0)	19.0(1.0)	17.6(1.0)	11.5(1.0)	11.1(1.0)
HTY[g]	35.0(1.0)	20.2(1.0)			
HSA1[h]	38.0(2.4)	20.8(2.3)	16.7(0.9)		
HSA2[i]	37.4(1.8)	22.2(0.8)	17.9(0.5)		
this work (0 K)[j]	32.4(1.4)	20.5(1.3)	16.7(1.3)	12.7(1.4)	12.2(1.8)
this work (E_{vib})[j]	32.1(2.5)	18.7(1.8)	14.4(1.4)	11.7(1.4)	13.0(1.4)
this work (298 K)[k]	30.1(2.3)	14.9(1.6)	9.1(1.0)	4.3(1.0)	4.5(0.7)

[a] Uncertainties are listed in parentheses. When uncertainties are not listed in the work referenced, we follow MS and use ±1.0 kcal/mol. [b] Reference 1. [c] Reference 2. [d] Reference 3. [e] Reference 6. [f] Reference 7. [g] Reference 8. [h] Reference 12. [i] Reference 13. [j] Based on the assumption that dissociation at the thresholds obtained here represents formation of products at 0 K. See text. [k] Based on the assumption that dissociation at the thresholds obtained here represents formation of products at 298 K. See text.

† Permanent address: Department of Material Science, Himeji Institute of Technology, Kamigoro, Hyogo, Japan 678-12.

* Abstract published in *Advance ACS Abstracts*, December 1, 1993.

(1) Kebarle, P.; Searles, S. K.; Zolla A.; Arshadi, M. *J. Am. Chem. Soc.* **1967**, *89*, 6393.
(2) Cunningham, A. J.; Payzant A. D.; Kebarle, P. *J. Am. Chem. Soc.* **1972**, *94*, 7627.
(3) Lau, Y. K.; Ikuta, S.; Kebarle, P. *J. Am. Chem. Soc.* **1982**, *104*, 1462.
(4) Kebarle, P.; Dillow, G. W.; Hirao, K.; Chowdhury, S. *Faraday Discuss. Chem. Soc.* **1988**, *85*, 1.
(5) Beggs, D. P.; Field, F. H. *J. Am. Chem. Soc.* **1971**, *93*, 1567.
(6) Meot-Ner, M.; Field, F. H. *J. Am. Chem. Soc.* **1977**, *99*, 998.
(7) Meot-Ner, M.; Speller, C. V. *J. Phys. Chem.* **1986**, *90*, 6616.
(8) Hiraoka, K.; Takimoto, H.; Yamabe, S. *J. Phys. Chem.* **1986**, *90*, 5910.
(9) Frisch, M. J.; Del Bene, J. E.; Binkley, J. S.; Schaefer, H. F., III *J. Chem. Phys.* **1986**, *84*, 2279.
(10) Dawson, P. H. *Int. J. Mass Spectrom. Ion Processes* **1982**, *43*, 195.
(11) Magnera, T. F.; David, D. E.; Michl, J. *Chem. Phys. Lett.* **1991**, *182*, 363.
(12) Honma, K.; Sunderlin, L. S.; Armentrout, P. B. *Int. J. Mass Spectrom. Ion Processes* **1992**, *117*, 237.
(13) Honma, K.; Sunderlin, L. S.; Armentrout, P. B. *J. Chem. Phys.* **1993**, *99*, 1623.
(14) Narcisi, R. S.; Bailey, A. D. *J. Geophys. Res.* **1965**, *70*, 3687.

0002-7863/93/1515-12125$04.00/0

$\Delta H°(x+1) - 2\Delta H°(x)$.[7] They find that $\delta\Delta H°(3)$ is less than zero, a result that suggests particular stability for the $H_9O_4^+$ cluster. This appears consistent with the so-called Eigen structure for this cluster: H_3O^+ surrounded by a complete solvent shell composed of three water molecules.

$H_3O^+(H_2O)_x$ clusters have also been studied by collision induced dissociation (CID) in triple quadrupole mass spectrometers by Dawson[10] and Magnera, David, and Michl (MDM).[11] Although Dawson's work provides no quantitative results for $\Delta H°(x)$, he does report good agreement with the accepted values of that time on the basis of retarding potential analysis curves. More recently, MDM have measured the differences between CID thresholds for the loss of one, two, three, and four water molecules from $H_3O^+(H_2O)_x$ (x = 2–27). Their measured bond energies are in qualitative agreement with the literature results for $x \leq 3$ given their estimated uncertainty of 1.5–3.0 kcal/mol, but their results are outside combined experimental error for x = 4 and 5. In addition, these results are for clusters at an unknown temperature so the comparison is imprecise and not definitive. Honma, Sunderlin, and Armentrout have recently published studies of $H_3O^+(H_2O)_x$ (x = 1–3) reacting with NH_3 (HSA1)[12] and CH_3CN (HSA2).[13] These studies report values for $\Delta H°(x)$, shown in Table I, as derived from threshold analysis of the CID channels in these systems. Both studies report significantly larger values than Kebarle and MS for $\Delta H°(1)$ and values that are in reasonable agreement for $\Delta H°(2)$ and $\Delta H°(3)$.

Because of the discrepancies in some of the recently measured hydration enthalpies, especially $\Delta H°(1)$, and the lack of reliable data by any method other than HPMS and its variants, we have undertaken to perform a definitive threshold CID study of the $H_3O^+(H_2O)_x$ systems. By using a protocol established in previous studies of metal–ligand complexes and covalently bound ions,[15-18] we obtain good agreement with literature thermochemistry. We thereby provide accurate values for $\Delta H°(x)$ by means other than the equilibrium method of HPMS and help to resolve discrepancies presently in the literature. Results obtained by using alternate assumptions regarding the proper interpretation of CID thresholds are also evaluated and found to yield thermochemistry inconsistent with previous results. In the context of CID studies, we also discuss the present results in relation to previous results from this laboratory and the work of MDM and Dawson.

Experimental Methods

General. Complete descriptions of the apparatus and experimental procedures are given elsewhere.[19,20] The production of proton bound water clusters is described below. Briefly, ions are extracted from the source, accelerated, and focused into a magnetic sector momentum analyzer for mass analysis. Mass-selected ions are slowed to a desired kinetic energy and focused into an octopole ion guide that radially traps the ions. The octopole passes through a static gas cell containing the xenon collision gas. After exiting the gas cell, product and unreacted beam ions drift to the end of the octopole where they are focused into a quadrupole mass filter for mass analysis and then detected. Ion intensities are converted to absolute cross sections as described previously.[19] Absolute uncertainties in cross sections are estimated as ±20%, and relative uncertainties are ±5%.

Laboratory ion energies are related to center-of-mass (CM) frame energies by $E(\mathrm{CM}) = E(\mathrm{lab})m/(M + m)$ where M and m are the ion and neutral reactant masses, respectively. Sharp features in the observed cross sections are broadened by the thermal motion of the neutral gas and the distribution of ion energies. The full width at half maximum (fwhm) of the neutral gas motion at nominal energy E_0(CM) is given by fwhm $\approx [11.1k_BTE_0M/(M + m)]^{1/2}$.[21] The fwhm of the ion beam energy distribution was typically between 0.2 and 0.6 eV lab for these experiments. The zero of the absolute energy scale and the ion energy distribution are measured by a retarding potential technique described elsewhere,[19] where we fit a Gaussian distribution to the derivative of the retarding potential curve. This allows the uncertainty in the absolute energy scale to be determined to within ±0.05 eV lab, which corresponds to 0.04 eV CM for x = 1 to 0.03 eV CM for x = 5. Because the energy analysis region and the reaction zone are physically the same, ambiguities in the energy analysis resulting from contact potentials, space charge effects, and focusing aberrations are minimized. Experiments conducted at low kinetic energies are consistent with absolute kinetic energies accurate within the cited uncertainty.[22,23]

Ion Source. The ions are formed in a 1 m long flow tube[20] operating at a pressure of 0.4–1.0 Torr with a helium flow rate of 3500–15000 standard cm³/min. In this source, He^+ and He^* are formed in a microwave discharge and react further downstream with H_2O added to the flow diluted by helium. Dissociative ionization and three-body collisions form the proton bound water clusters. As in the previous work of Honma, Sunderlin, and Armentrout,[12,13] we assume that the $H_3O^+(H_2O)_x$ clusters produced in this source are in their ground electronic states and that the internal energy of these clusters is well described by a Maxwell–Boltzmann distribution of rotational and vibrational states corresponding to 298 K. Previous work from this laboratory, including studies of N_4^+,[24] $Fe(CO)_x^+$ (x = 1–5),[15] $Cr(CO)_x^+$ (x = 1–6),[16] SiF_x^+ (x = 1–4),[17] and SF_x^+ (x = 1–5),[18] have shown that these assumptions are valid.

Thermochemical Analysis. Theory and experiment[25] have shown that cross sections can be modeled in the threshold region with eq 2,

$$\sigma = \sigma_0 \sum g_i (E + E_i + E_{\mathrm{rot}} - E_0)^n / E \qquad (2)$$

where σ_0 is an energy independent scaling factor, E is the relative translational energy of the reactants, E_{rot} is the rotational energy of the reactants,[26] E_0 is the threshold for reaction of the ground vibrational and electronic state, and n is an adjustable parameter. The summation is over i which denotes the vibrational and electronic states, g_i is the population of those states (Σg_i = 1), and E_i is the excitation energy of each specific state. Although no excited electronic states are believed to be present in these experiments, proton-bound water cluster ions have many low-frequency vibrational modes such that the populations of excited vibrational levels are not negligible at 298 K.

In the absence of evidence to the contrary, it is assumed that n and σ_0 in eq 2 are the same for all states. This form of eq 2 is expected to be appropriate for translationally driven reactions[27] and has been found to reproduce reaction cross sections well in a number of previous studies of both atom–diatom and polyatomic reactions,[28,29] including CID processes. In particular, cross sections for CID of N_4^+,[24] $Fe(CO)_x^+$ (x = 1–5),[15] $Cr(CO)_x^+$ (x = 1–6),[16] SiF_x^+ (x = 1–4),[17] and SF_x^+ (x = 1–5),[18] have been shown to be modeled well by eq 2 when reasonable values for vibrational frequencies are employed.

The model of eq 2 is convoluted with the kinetic energy distributions of the reactants,[19] and the parameters σ_0, n, and E_0 are optimized by using a nonlinear least-squares analysis to give the best fit to the data. An estimate of the error associated with the measurement of E_0 is obtained from the range of threshold values measured for different data sets with variations in the parameter n, variations associated with uncertainties in the vibrational frequencies, as discussed below, and the error in the absolute energy scale.

Vibrational frequencies used in eq 2 to model cross sections are listed in Table II. Two sets of *ab initio* harmonic vibrational frequencies for

(15) Schultz, R. H.; Crellin, K. C.; Armentrout P. B. *J. Am. Chem. Soc.* **1991**, *113*, 8590.
(16) Khan, F. A.; Clemmer, D. C.; Schultz, R. H.; Armentrout, P. B. *J. Phys. Chem.* **1993**, *97*, 7978.
(17) Fisher, E. R.; Kickel, B. K.; Armentrout, P. B. *J. Phys. Chem.* **1993**, *97*, 10204.
(18) Fisher, E. R.; Kickel, B. L.; Armentrout, P. B. *J. Chem. Phys.* **1992**, *97*, 4859.
(19) Ervin, K. M.; Armentrout, P. B. *J. Chem. Phys.* **1985**, *83*, 166.
(20) Schultz, R. H.; Armentrout, P. B. *Int. J. Mass Spectrom. Ion Processes* **1991**, *107*, 29.
(21) Chantry, P. J. *J. Chem. Phys.* **1971**, *55*, 2746.
(22) Ervin, K. M.; Armentrout, P. B. *J. Chem. Phys.* **1987**, *86*, 2659.
(23) Burley, J. D.; Ervin, K. M.; Armentrout, P. B. *Int. J. Mass Spectrom. Ion Processes* **1987**, *80*, 153. Sunderlin, L. S.; Armentrout, P. B. *Chem. Phys. Lett.* **1990**, *167*, 188.
(24) Schultz R. H.; Armentrout P. B. *J. Chem. Phys.* **1992**, *96*, 1046.
(25) See for example Aristov, N.; Armentrout, P. B. *J. Am. Chem. Soc.* **1986**, *108*, 1806.
(26) Conservation of the rotational energy of the reactants is not required here because CID is a bimolecular process. The rotational energy of the cluster after collision with the target gas is not neccesarily $3/2kT$, and in fact it could be either lower or higher.
(27) Chesnavich, W. J.; Bowers, M. T. *J. Phys. Chem.* **1979**, *83*, 900.
(28) See for example: Sunderlin, L. S.; Armentrout, P. B. *Int. J. Mass Spectrom. Ion Processes* **1989**, *94*, 149.
(29) Armentrout, P. B. In *Advances in Gas Phase Ion Chemistry*; Adams, N. G., Babcock, L. M., Eds.; JAI: Greenwich, 1992; Vol. 1, pp 83–119.

Table II. Vibrational Frequencies (cm^{-1}) and Average Energies at 298 K

species	E_{vib}, eV	frequencies (degeneracies)[a]
H_2O	0.0001	3756, 3652, 1595
H_3O^+	0.0015	3514(2), 3530, 1715(2), 910
$H_5O_2^+$ (HSA)[b]	0.043	4045, 4044, 3934, 3922, 1844, 1834, 1698(2), 690, 639, 601(2), 510(2), 214
$H_5O_2^+$ (FDBS)	0.052	3877(2), 3784, 3776, 1777, 1737, 1593, 1514, 805, 621, 549, 545, 470, 298, 175
$H_7O_3^+$ [b]	0.115	4086, 4083, 4034, 3962, 3961, 2755, 2629, 1871, 1828, 1801, 1779, 1405, 1261, 672, 561, 512, 478, 439, 412, 385, 374, 125, 107, 91
$H_9O_4^+$ [b]	0.202	4096(2), 4094, 3968, 3967, 3966, 3192, 3147, 3137, 1915, 1886, 1797, 1793, 1792, 1333, 1128, 1065, 826, 515, 511, 446, 431, 410, 394, 375, 374, 282, 129, 110, 91, 75, 74, 66
$H_{11}O_5^+$ [c]	0.289	$H_9O_4^+$ frequencies + 3968, 3192, 1793, 1065, 375, 282, 75(2), 66(2)
$H_{13}O_6^+$ [c]	0.375	$H_{11}O_5^+$ frequencies + 3958, 3192, 1793, 1065, 375, 282, 75(2), 66(2)

[a] From ref 9, except as noted. [b] Frequencies from ref 12. [c] Frequencies estimated from $H_9O_4^+$ frequencies. See text.

$H_5O_2^+$ were used. One is taken from HSA1[12] where the HONDO7 program employing a 4-31G basis set was used, while the other, calculated at the MP2/6-311++G(2d,2p) level, is from Frisch et al. (FDBS).[9] Vibrational frequencies for $H_7O_3^+$ and $H_9O_4^+$ are also taken from HSA1[12] and were calculated by using HONDO7. No scaling was applied to these ab initio frequencies before use because the level of theory applied in both cases should adequately describe the vibrations of a predominantly electrostatic interaction.[30] Although it would be appropriate to scale the internal modes of water, we have not done so here. This choice introduces a negligible error in the final results because the internal modes of water are too high in energy to make a significant contribution to the excited state population of the clusters at 298 K.

Vibrational frequencies used for $x = 4$ and 5 are the frequencies for $x = 3$ with estimates of the additional intermolecular modes included. However, treatment of the internal energy of the outermost water molecules does pose some difficulty. Poised at the periphery of the Eigen structure of $H_9O_4^+$, the outermost water molecules of $H_{11}O_5^+$ and $H_{13}O_6^+$ are hindered rotors in the low-temperature limit and free rotors in the high-temperature limit. Because we do not know with certainty that we are in the high-temperature limit with respect to the barrier to rotation of the outermost waters, we have added an additional uncertainty of $k_BT/2$, the difference between the heat capacity of a hindered rotor (k_BT) and a free internal rotor ($k_BT/2$), to the internal energy of this molecule.

Another interpretational difficulty arises when the calculated internal energy distribution includes states with energies exceeding the threshold for ligand loss. Experimentally, we do not observe dissociation of the parent ions in the absence of collision gas, i.e., there is no appreciable metastable dissociation of ions in the interaction region. Either such ions have dissociated before the initial mass selection or their lifetimes are sufficiently long that they survive more than the flight time through the entire instrument, hundreds of microseconds. If the lifetimes are short, it would be appropriate to truncate the internal energy distribution at the bond energy of the cluster; but if the lifetimes are long, these metastable ions must still be accounted for in the modeling process. One possibility would be to represent this fraction of the ion beam with an appropriately scaled ion–molecule collision cross section, but this approach is contradicted by the observation that this calculated cross section exceeds the cross sections measured at the lowest kinetic energies studied. Another possibility is to "pile-up" all of this population where $E_l + E_{rot} = E_0$ in eq 2, and this is the approach used here for all clusters. Because the fraction of the ion beam that could be metastable is quite small (generally less than 5%), we obtain no objective experimental information regarding the most correct interpretation. For the case of $x = 5$, where the potential problem is the most severe, 15% of the ion beam is calculated to be "metastable". The threshold obtained by excluding these ions totally differs from that obtained when these ions are included by only 0.01 eV. This problem promises to become more egregious as the clusters studied become larger and may eventually limit the applicability of the CID approach. A more definitive evaluation of the best experimental interpretation of CID thresholds for such clusters awaits such additional studies.

One final consideration in the analysis of CID thresholds is whether dissociation occurs within the time scale of the experiment, approximately 10^{-4} s in our instrument. If the lifetime of the collisionally excited clusters exceeds this, then the measured thresholds will be shifted to higher kinetic energies leading to a kinetic shift. We have previously detailed how to include consideration of this effect in our threshold analysis by incorporating RRKM theory into eq 2.[16,31] In the present study, we find no appreciable kinetic shifts for $H_3O^+(H_2O)_x$ ($x = 1$–3), while for $x = 4$, the shift is only 0.03 eV, and for $x = 5$, the shift is 0.06 eV. The thresholds determined below for $x = 4$ and 5 include these corrections, and the uncertainties in these values include the effects of varying the time scale (10^{-4} s) over a factor of 2.

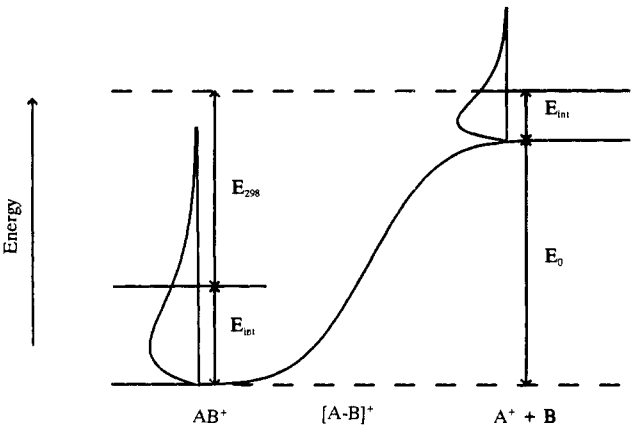

Figure 1. Qualitative potential energy surface as a function of reaction coordinate for the general dissociation reaction $AB^+ \rightarrow A^+ + B$. E_{int} represents the average internal energy of the indicated species at 298 K. Maxwell–Boltzmann shaped distributions are shown to emphasize that the internal energy of the reactants truly has a distribution, and that in the 298 K product model, the products are implicitly assumed to have a distribution of energies. The quantity labeled E_0 represents the minimum input of energy required for dissociation of reactants at 0 K. The arrow labeled E_{298} represents the minimum energy for dissociation under the 298 K product assumption.

Temperature Assumptions in the Thermochemical Analysis. The use of eq 2, which explicitly includes E_{rot} and E_l, to analyze the threshold behavior of CID cross sections makes the statistical assumption that the internal energy of the cluster is available to effect dissociation. This is appropriate for the *bimolecular* CID process because both rotational and vibrational energy of the reactants are redistributed throughout the cluster upon impact with the collision gas. (Also the bimolecular nature of CID allows angular momentum to be conserved at threshold by virtue of nonzero impact parameters compensating for collisions with rotating clusters.) If this model truly measures the threshold (the least amount of energy necessary) for dissociation, then this threshold must correspond to the formation of products with no internal energy. We have used this assumption and eq 2 in all our recent CID studies,[15–18] and refer to it here as the "0 K model". The situation is illustrated in Figure 1, where a qualitative potential energy surface for the dissociation of an ion–molecule complex is shown. No activation barrier in excess of the dissociation endothermicity is shown because this is generally true for ion–molecule reactions, as has been explicitly tested a number of times.[22,29,32] Figure 1 shows that E_0, the threshold defined in eq 2, is the energy needed to dissociate the reactant complex at 0 K. For reactants at 298 K (or any other temperature), this threshold is reduced by the explicit distribution

(30) Bauschlicher, C. W., Jr.; Langhoff, S. R.; Partridge, H.; Rice, J.; Komornicki, A. *J. Chem. Phys.* **1991**, *95*, 5142. Bauschlicher, C. W. Jr., personal communication.

(31) Loh, S. K.; Hales, D. A.; Lian, L.; Armentrout, P. B. *J. Chem. Phys.* **1989**, *90*, 5466.

(32) Boo, B. H.; Armentrout, P. B. *J. Am. Chem. Soc.* **1987**, *109*, 3459. Elkind, J. L.; Armentrout, P. B. *J. Phys. Chem.* **1984**, *88*, 5454. Armentrout, P. B. *Structure/Reactivity and Thermochemistry of Ions;* Ausloos, P., Lias, S. G., Eds.; D. Reidel: Dordrecht, 1987; pp 97–164.

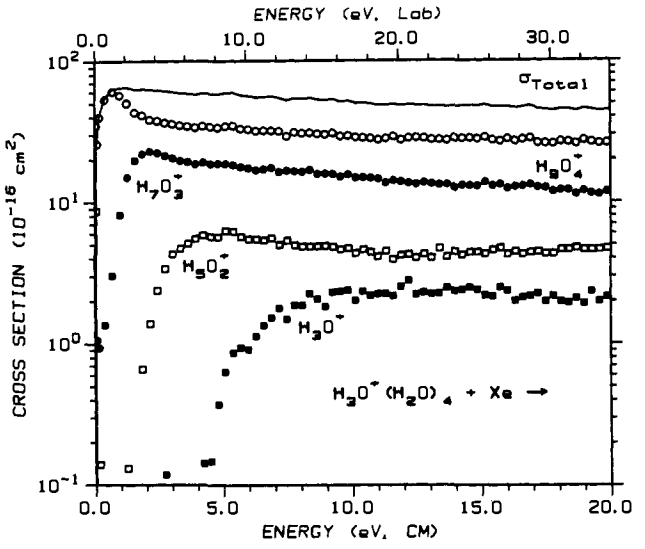

Figure 2. Cross sections for CID of $H_3O^+(H_2O)_4$ as a function of relative collision energy (lower x axis) and laboratory energy (upper x axis). The solid line shows the total cross section for dissociation.

of internal energies, E_{int}, equivalent to the sum of rotational (E_{rot}), electronic, and vibrational (E_l) energies in the reactants.

One might ask whether the use of the explicit *distribution* of vibrational energies is needed in eq 2. Would it be sufficient to drop the summation over E_l and replace this term with E_{vib}, the average vibrational energy of the $H_3O^+(H_2O)_x$ reactants at 298 K, as listed in Table II? Indeed, we have done this in eq 2 for the rotational energies, because this distribution is sufficiently narrow that the use of the average rotational energy is accurate. In the results section, we evaluate the accuracy of this simplification for the vibrational energy as well.

In the past, we and others have assumed (at some times implicitly) that dissociation at threshold corresponds to formation of products at 298 K, which we term the "298 K model" here. This model is equivalent to the assumption that the measured threshold is represented by E_{298} in Figure 1, and interprets the data by modifying eq 2 to eliminate E_{rot} and E_l. There are two possible rationales for this model. One, if rotational

$$\sigma = \sigma_0 (E - E_{298})^n / E \qquad (3)$$

and most vibrational modes are not coupled well with the dissociation coordinate, then products could be formed with energy retained in these modes at the same temperature as the reactants. Second, efficient formation of products may not begin until the products can be formed without transferring energy from these decoupled modes. In the results section, we model our data by using both eqs 2 and 3 and in order to test the validity of the 0 and 298 K models.

Results

Cross sections for CID of $H_3O^+(H_2O)_4$ with xenon at collision energies below 20 eV in the center of mass frame are shown in Figure 2. No product ions other than those shown were observed within the indicated experimental sensitivity. CID results for all other clusters studied were similar. The largest cross section observed in each of these systems corresponds to loss of a single water molecule, reaction 4.

$$H_3O^+(H_2O)_x + Xe \rightarrow H_3O^+(H_2O)_{x-1} + H_2O + Xe \qquad (4)$$

$$H_3O^+(H_2O)_x + Xe \rightarrow H_3O^+(H_2O)_{x-y} + yH_2O + Xe \qquad (5)$$

For all clusters, these cross sections rise from apparent thresholds lower than 1.0 eV. As the kinetic energy of the collision is increased, the cross sections reach maxima of 5 to 64 Å^2, Table III, and then diminish only slightly at higher energies. Cross sections corresponding to reaction 5, multiple water molecule loss, rise from thresholds higher than those of reactions 4, and remain smaller than the primary cross sections in all cases. Above about 10 eV, the branching ratios for each cluster system remain relatively constant and are listed in Table III.

Table III. Total Cross Sections and Branching Ratios of Reactions 5

		branching ratio for loss of y water molecules[b]				
x	σ_{total},[a] Å^2	1	2	3	4	5
1	3	1.00				
2	22	0.80	0.20			
3	26	0.78	0.15	0.07		
4	47	0.58	0.28	0.09	0.05	
5	49	0.44	0.37	0.10	0.07	0.02

[a] Uncertainties are ±20%. [b] Uncertainties are ±0.02.

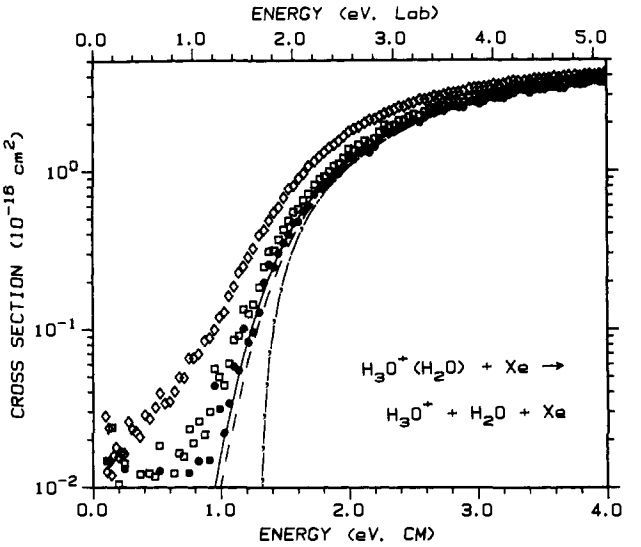

Figure 3. Cross section for CID of $H_5O_2^+$ with Xe to form H_3O^+ as a function of relative kinetic energy (lower x axis) and laboratory kinetic energy (upper x axis). Open diamonds and open squares show the cross sections measured at P(Xe) = 0.40 and 0.08 mTorr, respectively. Closed circles show these cross sections extrapolated to P(Xe) = 0.00 mTorr. The best fit of eq 2 to the zero pressure cross section (dashed line) is shown convoluted over neutral and ion kinetic energy distributions (solid line). The dash-dot line shows the model cross section in the absence of experimental kinetic energy broadening for reactants with an internal temperature of 0 K.

Examination of the branching ratios in Table III shows that the loss of one water molecule dominates the product spectrum for most clusters. The exception is the $H_3O^+(H_2O)_5$ cluster, which shows nearly equal efficiency for the loss of one and two water molecules. This may be evidence that $H_3O^+(H_2O)_3$ has some special thermodynamic stability, but it may also be simply a reflection that the two outermost water molecules of the x = 5 cluster are bound less strongly than those for the smaller clusters.

Pressure Effects. Equations 2 and 3 only model cross sections that represent products formed as a result of a single collision. In the present experiments, the pressure of the xenon collision gas, P(Xe), is generally kept sufficiently low that multiple collisions with the ions are rare, but even under such conditions, the effects of multiple collisions can be significant. This is illustrated in Figure 3, which shows representative data for CID of $H_5O_2^+$ collected with P(Xe) ≈ 0.40 mTorr and P(Xe) ≈ 0.08 mTorr. It can be seen that the apparent threshold for dissociation shifts to lower energy as the pressure of xenon is increased. We have verified that such pressure effects become more pronounced for $H_7O_3^+$ and $H_9O_4^+$, an observation that is similar to our work on transition metal clusters.[33,34] In addition, we note that the

(33) Hales, D. A.; Lian, L.; Armentrout, P. B. *Int. J. Mass Spectrom. Ion Processes* **1990**, *102*, 269.
(34) Lian, L.; Su, C.-X.; Armentrout, P. B. *J. Chem. Phys.* **1992**, *96*, 7542; *97*, 4072, 4084.

Table IV. Parameters of Eqs 2 and 3 Used To Analyze CID Cross Sections[a]

x	model[b]	E_T,[c] eV	n	σ_0
1	0 K (FDBS)	1.36(0.04)	1.5(0.1)	4.0(0.2)
	0 K (FDBS, ×2)[d]	1.33(0.04)	1.4(0.1)	4.0(0.1)
	0 K (FDBS, ×1/2)[e]	1.38(0.04)	1.5(0.1)	4.1(0.1)
	0 K (HSA)	1.33(0.06)	1.5(0.1)	3.6(0.2)
	0 K, E_{vib}	1.32(0.11)	1.4(0.1)	4.9(0.7)
	298 K	1.28(0.10)	1.4(0.1)	4.9(0.7)
2	0 K	0.86(0.06)	1.5(0.2)	18.6(0.8)
	0 K, E_{vib}	0.74(0.08)	1.6(0.2)	17.2(1.4)
	298 K	0.62(0.07)	1.6(0.2)	17.2(1.4)
3	0 K	0.71(0.06)	1.2(0.3)	38.6(2.8)
	0 K, E_{vib}	0.57(0.06)	1.5(0.2)	36.9(0.8)
	298 K	0.37(0.04)	1.5(0.2)	36.9(0.8)
4	0 K	0.52(0.06)	0.9(0.1)	62(5)
	0 K, E_{vib}	0.49(0.06)	1.1(0.1)	56(5)
	298 K	0.16(0.04)	1.1(0.1)	56(5)
5	0 K	0.51(0.08)	0.9(0.1)	86(8)
	0 K, E_{vib}	0.54(0.06)	0.9(0.1)	75(6)
	298 K	0.17(0.03)	0.9(0.1)	75(6)

[a] Uncertainties are listed in parentheses. [b] See the text for a description of the various models employed to interpret the data. The vibrational frequences used are taken from Table II. [c] E_T equals E_{298} for the 298 K model and E_0 otherwise. [d] FDBS intermolecular vibrational frequencies multiplied by 2. [e] FDBS intermolecular vibrational frequencies divided by 2.

models of eqs 2 and 3 cannot reproduce the experimental cross sections taken at elevated pressures.

In order to circumvent this problem, we collect data at two or more pressures and then extrapolate the data to zero pressure.[15,33] Several data sets are collected with a low pressure of xenon, typically $P(Xe) \approx 0.05$ mTorr, and several data sets are collected with $P(Xe)$ as high as possible without attenuating the reactant ion beam intensity by more than 10%, ~0.15 mTorr for $x = 2$ and 3. Each pair of high- and low-pressure cross sections are linearly extrapolated to zero pressure, rigorously single collision conditions, at each energy. Figure 3 clearly shows that such an extrapolation has an apparent threshold that is still higher than that of the lowest pressure data. The thresholds reported for $x = 1$–3 in this work are determined from data extrapolated to zero pressure in this manner. Interestingly, thresholds for dissociation of the $x = 4$ and 5 clusters show no obvious evidence of the effects of multiple collisions. This observation appears to be due to the very low threshold energies, such that the cross sections for *single* collision CID are nonzero at all energies, leaving no energy region where the effects of multiple collisions are important. The thresholds for dissociation of $x = 4$ and 5 are determined from data at 0.02–0.09 mTorr. Because the magnitude of the pressure effect is difficult to predict, careful pressure dependent studies of a cross section should always be performed to verify that the data are free from systematic errors induced by multiple collisions.

Vibrational Frequencies. The zero-pressure extrapolated cross sections for the $H_5O_2^+$ system were modeled with eqs 2 and 3 and the average optimum parameters are listed in Table IV. Figure 3 shows that the eq 2 model using the FDBS set of vibrational frequencies reproduces the zero-pressure cross section well. To estimate the sensitivity of the least squares optimization of σ_0, E_0, and n to the frequencies employed, the data were also modeled with the intermolecular vibrational frequencies of the FDBS set doubled and halved. This yields variations in the threshold of ±0.03 eV (Table IV), which we take to be a generous estimate of the uncertainties resulting from inaccurate frequencies. Use of the HSA frequencies yields a result differing from that obtained with the FDBS frequencies by only 0.03 eV. This good agreement is evidence that the HSA frequencies, calculated at a lower level of theory, are adequate for use in this analysis in comparison to the presumably more accurate FDBS frequencies. We take as our best measure of this threshold the average of the 0 K values in Table IV, $E_0 = 1.35 \pm 0.06$ eV.

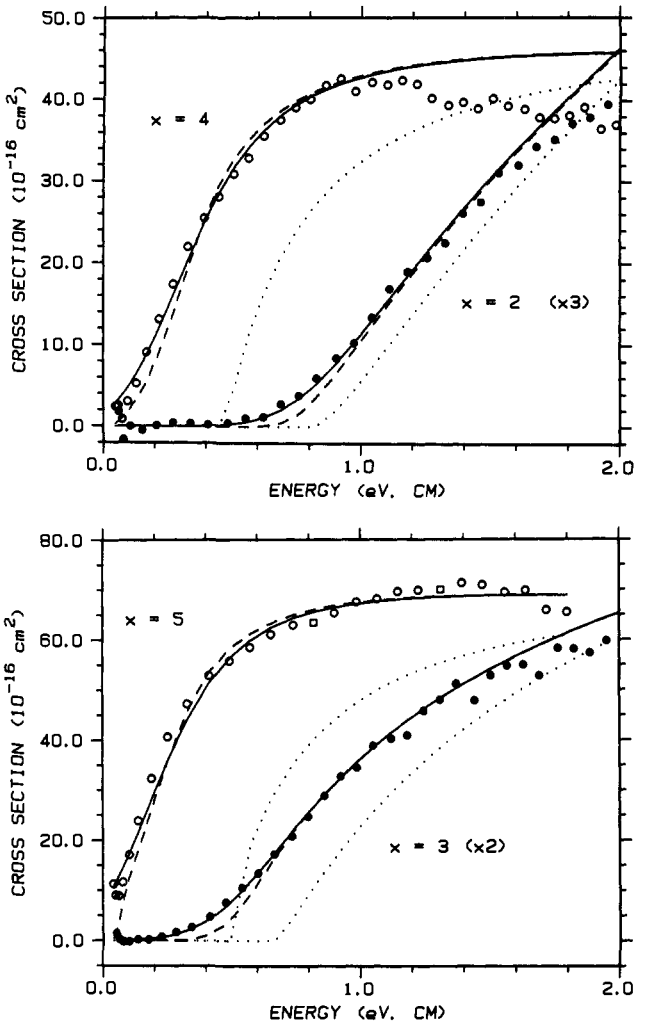

Figure 4. Threshold for the total CID cross sections, reaction 5, for $H_3O^+(H_2O)_x$ as a function of relative kinetic energy. Part a (top) shows results for $x = 2$ and 4 as closed and open circles, respectively, while part b (bottom) shows results for $x = 3$ and 5 as closed and open circles, respectively. The best fits of eq 2 are shown as dashed lines, and solid lines show these results convoluted over the neutral and ionic kinetic energy distributions. Dotted lines show the model cross sections in the absence of experimental kinetic energy broadening for reactants with an internal temperature of 0 K.

For the larger clusters ($x = 2$–5), there are no frequency sets calculated at higher levels of theory. Therefore, we proceed by using frequencies derived as discussed above and listed in Table II. We estimate the uncertainty in the thresholds resulting from the use of calculated frequencies as ±0.04 eV. This is larger than the difference between the average vibrational energy at 298 K when the intermolecular vibrational frequencies are halved and doubled.

Data Analysis. Between four and seven zero-pressure extrapolated cross sections were analyzed for the primary CID channels of $H_3O^+(H_2O)_x$ ($x = 1$–5) + Xe, reactions 4. For $x = 4$ and 5, the total cross sections are analyzed in order to avoid the need to reproduce changes in the cross section shape due to loss of the second water molecule. These secondary processes in the CID of $H_3O^+(H_2O)_x^+$ ($x = 1$–3) rise from sufficiently high thresholds that loss of the first water molecule corresponds to the total cross section over the entire energy range analyzed.

For all clusters, the cross sections were analyzed with the 0 K model (eq 2), the 298 K model (eq 3), and the 0 K model after correcting by the average vibrational energy, E_{vib}. The best fit parameters for each model are listed in Table IV. The 0 K models are shown in Figures 3 and 4 and can be seen to reproduce the data well. The measured threshold and the parameter n both

decrease as the size of the cluster increases. This observation is not uncommon and reflects the tendency of n to approach a value of $^1/_2$ as the ion–molecule reaction becomes thermoneutral.[29,35] The 298 K and E_{vib} models (which are identical) do not reproduce the shape of the data as well. This is because the distribution of vibrational energies introduces curvature in the experimental cross sections. The 298 K and E_{vib} models try to reproduce this by allowing the parameter n to increase, but this cannot adequately represent the shape of the cross section as well as when the vibrational distribution is explicitly considered. Similar conclusions have been drawn elsewhere.[15,29]

Cross sections corresponding to multiple ligand loss are not analyzed because they have an intrinsically poorer signal-to-noise ratio compared with the primary channels. Further, there exists the possibility that these thresholds may be shifted to higher energies by kinetic and competitive shifts.[15,16] In addition, the thresholds may be lowered due to the possibility that H_2O molecules are lost as dimers or trimers. Thresholds affected by dimer loss would be lowered by the dimerization energy of water at 0 K, calculated to be about 3 kcal/mol.[9,36]

Discussion

Determination of Hydration Enthalpies. It seems reasonable that the dissociation of proton-bound water clusters should have no barriers to reactions 4 in excess of the bond dissociation energies because these are simple bond fission reactions in an ion–molecule system.[29,32] Given this assumption, the thresholds measured here can be equated with $D[H_3O^+(H_2O)_{x-1}–H_2O] = D(x)$. From the 0 K and E_{vib} (the explicit vibrational distribution and the average vibrational energy) models, we obtain 0 K bond energies, $D_0(x)$, as illustrated in Figure 1. These bond dissociation energies can then be converted to $\Delta H°(x)$ values at 298 K by eq 6,

$$\Delta H°(x) = D_0(x) - E_{vib}(x) + E_{vib}(x-1) + E_{vib}(H_2O) + 4k_BT \quad (6)$$

where $E_{vib}(x)$ is the average vibrational energy of $H_3O^+(H_2O)_x$ at 298 K. The $4k_BT$ term accounts for three translational and three rotational degrees of freedom created during the bond breaking process and the $\Delta PV = k_BT$ work term that converts energy to enthalpy. From the 298 K model, the thresholds correspond to $D_{298}(x)$ and can be converted to $\Delta H°(x)$ by adding only the ΔPV term. Hydration enthalpies at 298 K derived in this fashion from these three models are listed in Table I.

Comparison with Equilibrium Data. $\Delta H°(x)$ values obtained with the 0 K model show excellent agreement with Kebarle's best series (CPK and LIK)[4] and MS,[7] Table I and Figure 5. Our numbers differ from those of Kebarle by an average absolute magnitude of 0.7 ± 0.5 kcal/mol and from those of MS by an average absolute magnitude of 1.1 ± 0.3 kcal/mol. These discrepancies are well within the experimental errors of either type of experiment.

$\Delta H°(x)$ values obtained with the 298 K model are in exceptionally poor agreement with the literature data, providing strong empirical evidence that the 298 K model is invalid. The discrepancy increases with increasing cluster size and tracks reasonably well with the concomitantly increasing internal energy, a further indication that the 0 K model is physically correct.

$\Delta H°(x)$ values obtained with the E_{vib} model are in reasonable agreement with the literature data, except for $\Delta H°(3)$ where the deviation exceeds even the combined experimental errors. Such deviations can occur because in fitting the data without the explicit distribution of internal energies, the parameter n is forced to account for this distribution, as noted above. As a consequence, the shift in the measured thresholds between analyses with and without the internal energy distribution will generally exceed the

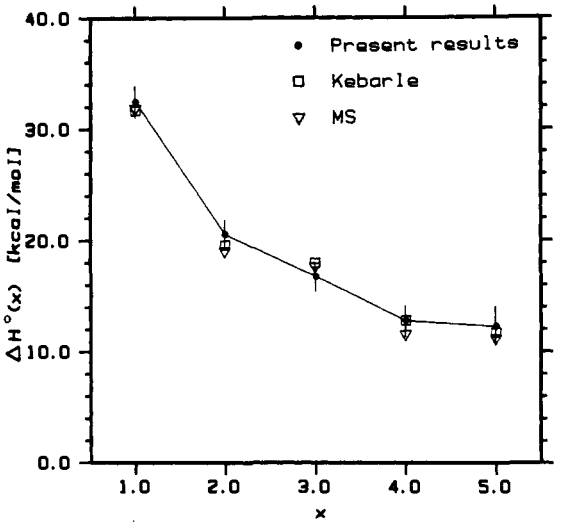

Figure 5. $\Delta H°(x)$ vs cluster size, x. The results of Kebarle[2,3] are shown as open squares, the results of MS[7] are shown as open triangles, and the present results obtained by using the 0 K model are shown as solid circles with uncertainties indicated as vertical lines.

average internal energy.[15,29] The magnitude of this shift depends on the detailed kinetic energy dependence of the cross section and cannot be predicted *a priori*. Thus, correcting CID thresholds by the average internal energy of the reactants does provide more accurate thermodynamic data than ignoring this energy (the 298 K model), but an explicit calculation of the internal energy distribution provides the most accurate thermochemistry and best reproduction of the data.

Evidence for Solvent Shell Formation. As noted above, $H_3O^+(H_2O)_5$ is observed to lose two water molecules more readily than any other cluster. Because the product formed is $H_3O^+(H_2O)_3$, this observation appears consistent with the belief that this species is particularly stable due to the filling of the first solvent shell. More direct information regarding such stability comes from the data of Kebarle and MS, which show steps in the $\Delta H°(x)$ values between $x = 3$ and 4, Figure 5, although MS point out that within their experimental error, the $\Delta H°(x)$ (x = 2–4) values could decline linearly. In fact, our results show such a linear decrease, Figure 5, although there could be a step within the experimental error of our measurements.

To help quantify a criterion for shell filling, MS suggest that values of $\delta\Delta H°(x)$, as defined in the introduction, below –2 kcal/mol indicate shell filling and values between –2 and 0 kcal/mol are a tentative sign of shell filling, where 2 kcal/mol is the propagated standard deviation from $\Delta H°(x)$ for the equilibrium experiments. The results of both Kebarle and MS provide clear evidence for shell filling at $x = 3$, $\delta\Delta H°(3)$ values of –3.6 ± 2 and –4.7 ± 2 kcal/mol, respectively, while the $\delta\Delta H°(3)$ value calculated from our results is only –0.2 ± 2.6 kcal/mol, still within combined experimental errors of $\delta\Delta H°(3)$ values from both Kebarle and MS. However, we note that the $\delta\Delta H°(x)$ values reach a local minimum for $x = 3$ for all three sets of experimental enthalpies. We suggest that this may be a more useful criterion to evaluate the relative stabilities of various clusters, especially for proton-bound clusters where changes in binding enthalpies due to solvent shell filling may be modest because the bonding is dominated by the extended hydrogen bonding network.

Comparison with Previous CID Results. The values obtained for $\Delta H°(2)$ and $\Delta H°(3)$ here and by HSA[12,13] are in good agreement, but HSA obtain $\Delta H°(1) = 38.0 \pm 2.4$ and 37.4 ± 1.8 kcal/mol, 5.6 ± 2.8 and 5.0 ± 2.3 kcal/mol larger than the 32.4 ± 1.4 kcal/mol value determined here. This is well outside the combined experimental error. A careful examination of representative data from both these systems finds that the threshold behavior for the CID of $H_5O_2^+$ by NH_3 and CH_3CN

(35) Ervin, K. M.; Armentrout, P. B. *J. Chem. Phys.* **1987**, *86*, 2659.
(36) Del Bene, J. E.; Mettee, H. D.; Frisch, M. J.; Luke, B. T.; Pople, J. A. *J. Phys. Chem.* **1983**, *87*, 3279.

is consistent with the present results, but that the cross sections rise more slowly than the CID cross sections measured here. There are two possible explanations for this effect. First, HSA pointed out that the CID thresholds in the systems they studied, $H_3O^+(H_2O)_x + NH_3$ and CH_3CN, could be affected by the other reaction channels (solvent exchange reactions) that have very large cross sections at the energies corresponding to the threshold for dissociation of $H_5O_2^+$. Second, the use of a polyatomic molecule to induce dissociation may be less efficient than the use of an atomic reagent because energy can be deposited in internal modes of the polyatomic collision gas. Overall, we conclude that the present value represents the best determination of $\Delta H°(1)$ from our laboratory.

We note that this change in $\Delta H°(1)$ from those determined in HSA1 and HSA2 influences the proton affinities (PAs) measured in these papers.[12,13] By using the $\Delta H°(1) = 32.4$ kcal/mol value determined here, we find that thresholds measured there lead to $PA(NH_3) = 205 \pm 4$ kcal/mol and $PA(CH_3CN) = 188.0 \pm 2.8$ kcal/mol, in good agreement with literature values.[37-39] This is further indication that the value of $\Delta H°(1)$ determined here is probably our most reliable.

A number of qualitative comparisons can be made between the present results and the early CID study of proton-bound water clusters by Dawson.[10] We observe total cross sections for dissociation (measured well above threshold) that are considerably smaller than those of Dawson. Some of this difference could be due to different collision gases (Dawson employed argon and methane). Dawson also observes that the cross sections for loss of multiple water molecules can exceed that for loss of a single water molecule, while we observe $\sigma(x-1) > \sigma(x-2) > \sigma(x-3)$, Table III. We believe that both of these discrepancies are primarily due to multiple collisions occurring in the studies of Dawson. Although Dawson states "there was little dependence of threshold behavior on target density", this conclusion contrasts sharply with our observation of pressure effects, as characterized in Figure 3. In fact, careful examination of Figure 6 of Dawson's paper provides corroborating evidence that higher target gas pressures do lower the apparent CID threshold. The influence of multiple ion–molecule collisions can be seen by comparing the target densities used here to those used by Dawson. For $H_5O_2^+$, the highest pressure used here, $P(Xe) \sim 0.4$ mTorr where the effects of multiple collisions are evident, Figure 3, corresponds to a target thickness of 1.1×10^{14} atoms/cm^2, while for the larger clusters, the target thickness in our experiments did not exceed 0.4×10^{14} atoms/cm^2. When the dissociation branching ratios measured here are compared with those of Dawson for target thicknesses less than 1×10^{14} atoms/cm^2, where single collision conditions prevail, qualitative agreement is obtained.

Finally, the effects of multiple collisions with the target gas may also affect Dawson's conclusion that "the measured daughter ion energy distributions show that the dissociation process is dominated by glancing angle collisions". This is based on retarding potential analysis curves of the fragment ions for parent ions initially at 24 eV in the laboratory frame. Dawson observes that the fragment ions have energy distributions much slower than those of the parent ions, consistent with glancing collisions *or* with multiple collisions with the target gas. The energy distributions may also be adversely affected by the ability of a quadrupole to serve as a radial ion trap. In contrast to Dawson's conclusion, our observation that CID of the proton-bound water clusters is observed at the thermodynamic thresholds means that collisions with small impact parameters must play a significant role at the dissociation threshold because these are the most efficient collisions for conversion of kinetic energy to internal energy of the cluster.

Conclusions

In our recent study of the CID of $Fe(CO)_x^+$ ions,[15] we examined several systematic effects on deriving accurate thermodynamic information from CID thresholds. These effects include (a) highly excited reactant ions, (b) multiple collisions with Xe, (c) thermal energy of the reactant ions that might contribute to the measured thresholds, and (d) the lifetime of the dissociating ions. By using a protocol established in previous work that accounts for each of these factors, CID studies of $H_3O^+(H_2O)_x$ (x = 1–5) clusters provide solvation enthalpies that are in excellent agreement with those in the literature as determined exclusively by equilibrium mass spectrometric methods. Our results therefore contribute a definitive threshold CID study of proton-bound water clusters to the literature and provide a valuable, independent verification of the thermochemistry obtained by equilibrium measurements, Without such verification, the possibility of systematic errors attributable to either method would exist. Such good agreement with the literature values also further establishes the interpretation of CID thresholds described here as an accurate method for measuring successive cluster–ligand bond energies.

Acknowledgment. This work is supported by the National Science Foundation, Grant No. CHE 9221241. We thank the referees for several useful comments.

(37) Lias, S. G.; Liebman, J. F.; Levin, R. D. *J. Phys. Chem. Ref. Data* **1984**, *13*, 695.
(38) Meot-Ner, M.; Sieck, L. W. *J. Am. Chem. Soc.* **1991**, *113*, 4448.
(39) Szulejko, J. E.; McMahon, T. B. *Int. J. Mass Spectrom. Ion Processes* **1991**, *109* 279.